

Article

Experimental Study on Water Distribution and Droplet Kinetic Energy Intensity from Non-Circular Nozzles with Different Aspect Ratios

Zixin Wang¹, Yue Jiang^{1,*}, Jialing Liu¹, Hong Li¹ and Hao Li²¹ Research Centre of Fluid Machinery Engineering and Technology, Jiangsu University, Zhenjiang 212013, China² Institute of Farmland Irrigation, Chinese Academy of Agricultural Sciences, Xinxiang 453002, China

* Correspondence: jyfluid@ujs.edu.cn

Abstract: (1) Background: In sprinkler irrigation systems, the water distribution and droplet kinetic energy are affected by the shape of the nozzle. In this paper, the effects of working pressure and aspect ratio (L/D) of circular and non-circular nozzles (diamond and ellipse) on water distribution and droplet kinetic energy intensity were investigated; (2) Methods: The hydraulic performance of a PY15 impact sprinkler with circular and non-circular nozzles was assessed under different working pressures, and the droplet diameter, velocity, and kinetic energy intensity were measured by a 2D video disdrometer. Moreover, the coefficient of variation (CV) and form factor (β) were introduced to represent the water distribution and droplet characteristics; (3) Results: The results revealed that, under the same working pressure, the CV of the diamond nozzle was the smallest compared with that of the circular and elliptical nozzles, reflecting a more uniform water distribution. The uniformity of water distribution was the best when the L/D of the elliptical nozzle was the smallest. In general, the larger the outlet diameter, the larger the wetted radius and water application rate. In addition, the smaller the L/D , the smaller the peak water distribution value and the radial increase of the kinetic energy intensity of a single nozzle. The maximum droplet kinetic energy per unit volume of the elliptical nozzle was the smallest compared with that of the circular and diamond nozzles. The circular nozzle at 200 kPa and the diamond and elliptical nozzles at 100 kPa obtained the highest uniformity coefficients of combined kinetic energy intensity distribution, which were 55.93% (circular), 67.59% (diamond), and 57.78% (elliptical) when the combination spacings were 1.0 R, 1.1 R and 1.2 R, and 1.0 R, respectively. Finally, the fitting function of unit volume droplet kinetic energy, distance from the nozzle, L/D , and working pressure of non-circular nozzles was established, and a fitting coefficient of 0.92 was obtained, indicating that the fitting equation was accurate; (4) Conclusions: At low working pressures, the elliptic and diamond nozzles showed better water distributions than the circular nozzle. The distal average droplet diameters of the sprinkler with non-circular nozzles were found to be smaller than those produced by the circular nozzle.

Keywords: impact sprinkler; non-circular nozzle; water distribution; aspect ratio; 2D video disdrometer; droplet kinetic energy distribution



Citation: Wang, Z.; Jiang, Y.; Liu, J.; Li, H.; Li, H. Experimental Study on Water Distribution and Droplet Kinetic Energy Intensity from Non-Circular Nozzles with Different Aspect Ratios. *Agriculture* **2022**, *12*, 2133. <https://doi.org/10.3390/agriculture12122133>

Academic Editors: Vadim Bolshev, Vladimir Panchenko and Alexey Sibirev

Received: 6 October 2022

Accepted: 9 December 2022

Published: 12 December 2022

Publisher's Note: MDPI stays neutral with regard to jurisdictional claims in published maps and institutional affiliations.



Copyright: © 2022 by the authors. Licensee MDPI, Basel, Switzerland. This article is an open access article distributed under the terms and conditions of the Creative Commons Attribution (CC BY) license (<https://creativecommons.org/licenses/by/4.0/>).

1. Introduction

Sprinkler irrigation is an effective irrigation method used for reducing water use in agriculture. Sprinkler irrigation systems are generally composed of a water source, a water pump and power equipment, a water delivery pipeline system, and sprinklers. The sprinklers are key pieces of equipment for the implementation of sprinkler irrigation. Their performance not only directly affects the spraying quality, but is also related to the economy of the entire sprinkler irrigation system. Among them, sprinklers with non-circular nozzles can achieve a low-pressure uniform spray, and have the advantage of improving the atomization quality. Therefore, non-circular nozzles have been widely used in agricultural sprinkler irrigation fields [1,2].

Sprinkler hydraulic performance mainly depends on the wetted radius, flow rate, water application rate, uniformity, and droplet diameter [3–6]. Among them, the water application rate and uniformity of the radial water application profile of a sprinkler are important indicators for assessing the uniformity of irrigation property and water distribution, as well as important parameters for evaluating the advantages and disadvantages of sprinkler irrigation systems [7–9]. Bubenzer and Jones [10] reported that the damage degree of water droplets sprayed onto silty soil is a power function relationship between the kinetic energy of water droplets and the sprinkler water application rate. Mohammed and Kohl [11] investigated the distribution trend of the kinetic energy per unit volume of a full-jet nozzle under multiple pressure levels, and revealed that the kinetic energy per unit volume of water droplets along the radial direction increases with decreasing pressure. Christiansen [12] proposed an equation for calculating the uniformity coefficient. El-Wahed et al. [13] surveyed the effects of sprinkler spacing, sprinkler height, and working pressure of a central pivot irrigation system on parameters such as the uniformity coefficient, low value distribution uniformity, and variation coefficient, and determined the best operation condition scheme to reduce the operation costs.

In addition, the droplet diameter, droplet velocity, and droplet kinetic energy of sprinkler irrigation are also important indicators for evaluating the hydraulic performance of a sprinkler, and have an important impact on sprinkler irrigation system quality [14–16]. Xu et al. [17] investigated droplet diameter distribution and developed a normal distribution model, square-root-normal distribution model, logarithmic normal distribution model, and upper limit logarithmic normal distribution model of droplet diameter. Gong et al. [18] used a 2D video disdrometer (2DVD) to study the distribution range of a NelsonD3000 nozzle under different pressure levels, the changing trend of drop diameter, as well as the relationship between drop velocity, angle, and drop diameter. Their results demonstrated that the water droplet diameter and range conformed to the exponential function relationship, and the velocity of water droplets increased logarithmically with the increase of water droplet diameter. Lorenzini [19] investigated the trends of droplet velocity and evaporation under different working pressure levels during sprinkler irrigation. Their results indicated that the air temperature has a significant effect on droplet evaporation, while the air friction should not be mistakenly ignored when calculating droplet evaporation. Ouazaa et al. [20] analyzed the velocity and kinetic energy of droplets using a ballistic model. The results revealed that, under the working pressures of 138 kPa and 69 kPa, the kinetic energy dissipation decreased with increasing nozzle diameter. Yan et al. [4] also analyzed droplet velocity and kinetic energy by using a ballistic model, and reported that the runoff rate, bulk density of soil surface crust, and sediment yield were generally directly proportional to the droplet kinetic energy flux density (DE f) values, while the initiation of runoff, infiltration rate, and infiltration depth prior to runoff were inversely proportional to DE f. Zhu et al. [21] researched single droplet kinetic energy, droplet kinetic energy per unit volume, kinetic energy intensity distribution trend, and the kinetic energy intensity uniformity coefficient under different combination spacings of a full-jet nozzle. The results showed that the relationship between the kinetic energy distribution of a single water droplet and the water droplet diameter in the full-jet nozzle fit well with the developed model and exhibited a power function relationship. Li and Ma [22] investigated the droplet kinetic energy distribution at different measurement points of square and circular nozzles using the flour method and the droplet equation of motion, and analyzed the relationship between nozzle shape and droplet kinetic energy. Moreover, a regression equation able to estimate the total kinetic energy of water droplets from medium-pressure nozzles based on the median diameter was obtained.

The shape of conventional sprinkler nozzles is circular. The newly introduced non-circular nozzles have the advantages of improved water distribution and spraying uniformity, as well as better hydraulic performance under low pressure compared with circular nozzles [23,24]. Wei et al. [25] conducted experiments on the hydraulic performance of non-circular and circular nozzles, produced contour maps of water distribution for a single

sprinkler, and obtained the corresponding range values based on water distribution. Chen et al. [2] investigated the effect of the shape coefficient of four different-shaped non-circular nozzles, i.e., diamond, semicircle + triangle, semicircle + rectangle, and star, on droplet diameter, and concluded that the droplet diameter in the end decreases with the increasing shape coefficient. Li et al. [26] experimentally analyzed and discussed the effects of non-circular nozzle shape and pressure on the shape change of a low-pressure jet, as well as the effects of nozzle outlet shape, working pressure, and inlet angle on the shape change of the jet. Zhou et al. [27] designed a variety of non-circular nozzles with the same area, experimentally investigated the uniformity of radial water application profile of the sprinkler, and found that the combined uniformity coefficient of the non-circular nozzles was significantly higher than that of circular nozzles. Jiang et al. [28] used high-speed photography to study the fracture and flow characteristics of non-circular nozzles, and revealed that, under the same working pressure, the triangular jet had the shortest fracture length and jet diffusion angle. Due to the different jet patterns produced by non-circular nozzles, their hydraulic performance is improved under low pressure. While the wetted radius of non-circular nozzles is reduced compared with that of circular nozzles, uniformity of the radial water application profile of the sprinkler is higher and the water droplet distribution is more uniform under low working pressure.

According to the above literature review, it can be understood that, due to their special geometric structure, non-circular nozzles have various jet shapes, which can reduce working pressure and improve their hydraulic performance. A quantitative study on the droplet distribution characteristics of non-circular nozzles under different working pressure levels will provide theoretical support for the application of non-circular nozzles. Nevertheless, there are only a few existing studies concerning the radio water distribution and water droplet kinetic energy distribution characteristics of non-circular nozzles with different aspect ratios (L/D : long axis/minor axis). Furthermore, no study has focused on the direct effect relationship between L/D , radio water distribution, and water drop kinetic energy. Consequently, in this paper, taking the non-circular nozzle as the research object, three types of nozzles with different shapes are designed, and the radial water distribution and kinetic energy intensity of non-circular nozzles with different aspect ratios under different working conditions are calculated. A 2DVD is used to test the water diameter and velocity of the non-circular nozzles. The distribution trend of the water drop kinetic energy is calculated, and the relationship between L/D , water distribution, and water drop kinetic energy is explored. In addition, the influence rule of water distribution and water drop distribution characteristics on nozzle hydraulic performance is determined, and a theoretical basis for further improving the spraying performance and studying the hydraulic characteristics of the nozzle outflow field is provided.

2. Materials and Methods

2.1. Non-Circular Nozzle Design

As shown in Figure 1, a common circular nozzle structure was taken as reference. d_0 is its outlet diameter, which was set as 4 mm, 5 mm, and 6 mm. Since the outlet section shape and outlet diameter of non-circular nozzles have an impact on the hydraulic performance of the sprinkler, the non-circular nozzles with elliptical and diamond shapes were designed to have the same flow rate. The non-circular nozzles with different aspect ratios are displayed in Figure 2, and the detailed structural parameters are given in Table 1.

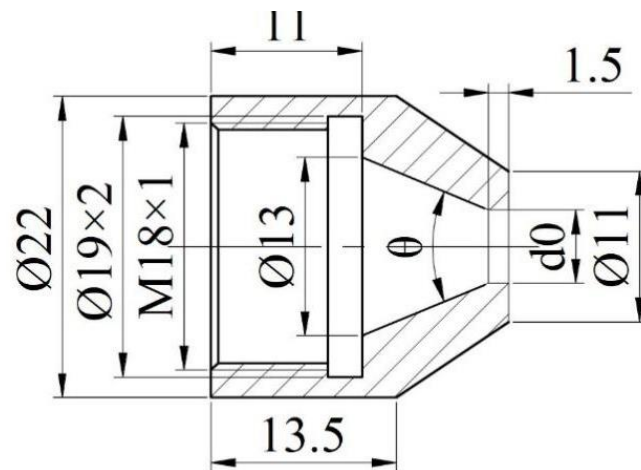


Figure 1. Schematic diagram (cross-section) of a circular nozzle structure with dimensions (mm).

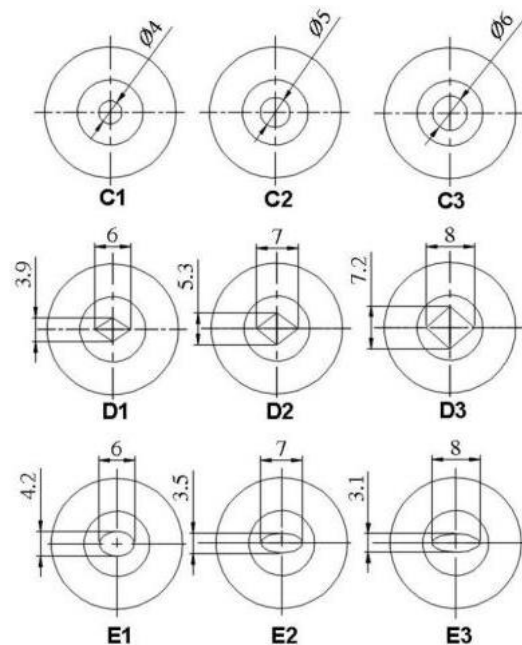


Figure 2. Schematic diagram (right view) of the investigated non-circular nozzles with dimensions (mm).

Table 1. Geometric parameters of the circular and non-circular nozzles (mm).

Inlet Cone Angle	Shape	Number	Outlet Diameter	Long Axis	Minor Axis	Aspect Ratio (L/D)
45°	Circle	C1	4	/	/	/
		C2	5	/	/	/
		C3	6	/	/	/
	Diamond	D1	4	6	3.9	1.54
		D2	5	7	5.3	1.32
		D3	6	8	7.2	1.11
	Ellipse	E1	5	6	4.2	1.43
		E2	5	7	3.5	2
		E3	5	8	3.1	2.58

In this paper, a PY15 impact sprinkler produced by Jinlong Spray Irrigation Co., China, was used for the experiments. The PY15 nozzle is a rotary impact nozzle with an inlet

diameter of 15 mm, working pressure of 200~400 kPa, nozzle diameter of 4~6 mm, and a jet elevation angle of 23°. Each nozzle was manufactured by a wire-cut electric discharge machining (EDM) process and was made of aluminum (Figure 3). Considering the error problem, flow error tests were performed after processing. It was found that the flow error of the nozzles with the same inlet cone angle and outlet diameter was less than 4% under the same pressure level (Table 2). Thus, it was considered that all nozzles followed the same flow principle.



Figure 3. Photograph of the sprinkler and nozzles used in experiments.

Table 2. Flow error analysis of equivalent-flow nozzles (the units of flow: m³/h).

Outlet Diameter	Number	150 kPa	200 kPa	250 kPa	300 kPa	350 kPa	400 kPa
5 mm	C2	1.067	1.234	1.385	1.516	1.636	1.747
	D2	1.036	1.198	1.347	1.476	1.601	1.709
	Difference	0.031	0.036	0.038	0.04	0.035	0.038
	Error	2.91%	2.92%	2.74%	2.64%	2.14%	2.18%
	E1	1.035	1.207	1.353	1.485	1.604	1.715
	Difference	0.032	0.027	0.032	0.031	0.032	0.032
	Error	3.00%	2.19%	2.31%	2.04%	1.96%	1.83%
	E2	1.075	1.261	1.411	1.554	1.673	1.79
	Difference	0.008	0.027	0.026	0.038	0.037	0.043
	Error	0.75%	2.19%	1.88%	2.51%	2.26%	2.46%
	E3	1.064	1.237	1.386	1.523	1.642	1.755
	Difference	0.003	0.003	0.001	0.007	0.006	0.008
Error	0.28%	0.24%	0.07%	0.46%	0.37%	0.46%	
4 mm	C1	0.693	0.81	0.898	0.981	1.067	1.142
	D1	0.675	0.78	0.88	0.975	1.052	1.131
	Difference	0.018	0.03	0.018	0.006	0.015	0.011
	Error	2.60%	3.70%	2.00%	0.61%	1.41%	0.96%
6 mm	C3	1.461	1.694	1.895	2.079	2.247	2.401
	D3	1.487	1.726	1.926	2.118	2.288	2.453
	Difference	0.026	0.032	0.031	0.039	0.041	0.052
	Error	1.78%	1.89%	1.64%	1.88%	1.82%	2.17%

2.2. Experimental Equipment

A 2DVD system manufactured by Joanneum Research Co., Graz, Styria, Austria, was employed to measure the size, shape, direction, aggregation state, and falling velocity of single droplets. The 2DVD system comprised two subsystems. The imaging system is composed of two background illumination sources, two line-scan cameras, and other components (Figure 4). The number of pixels of the camera was 512. The test area was 10,000 mm² (100 × 100 mm). The particle diameter measurement range was 0.2–8.0 mm and the vertical particle velocity range was 0–10.0 m/s. The data analysis and display system consisted of the View_HYD software (v8.010) designed by Joanneum Research Co., Graz, Styria, Austria, which was used to display the data generated by the 2DVD, record the measured droplet volumes, and calculate the rainfall velocity.



Figure 4. 2DVD system used to measure the characteristics of rainfall drops.

2.3. Test Method

The water flow distribution and droplet kinetic energy distribution experiments were performed in an indoor no-wind sprinkler irrigation hall with a diameter of 44 m. The PY15 impact sprinkler installation height was 1.4 m. Full-round spraying took place under the working pressure levels of 100 kPa, 150 kPa, 200 kPa, 250 kPa, and 300 kPa. Since there was no wind in the sprinkler hall, the instruments were placed along a linear path (ray). The data collected on this ray could be used to represent the data over the entire rotation. As it can be seen in Figures 5 and 6, rain gauges (opening diameter 85 mm) were placed in the radial direction of the jet at 1.0 m intervals. In order to ensure that the collected water would not overflow, the rain gauge was designed as a cylinder with a wedge-shaped opening edge without any defects. The test started after 10 min to ensure stable operation, and lasted for 1 h to determine the water application rate at each point. In addition, after the nozzle operated stably for 10 min, the 2DVD was moved by a distance of 2.0 m, and the diameter and velocity at each point were measured successively. The test duration at each point was at least 5 min. This is to ensure that the number of water droplets collected at each test location is higher than 5000, which is enough to provide appropriate water droplet statistics. In order to reduce the random and edge effect measurement errors caused by droplet splashing, the 3σ criterion of the normal distribution law of random errors is adopted to statistically test the particle number corresponding to the velocity value in each diameter range [29]. According to the relationship between droplet diameter and droplet falling speed, the diameter range was determined, so as to identify and eliminate the gross error, and then, the spray water drop strike kinetic energy was calculated.

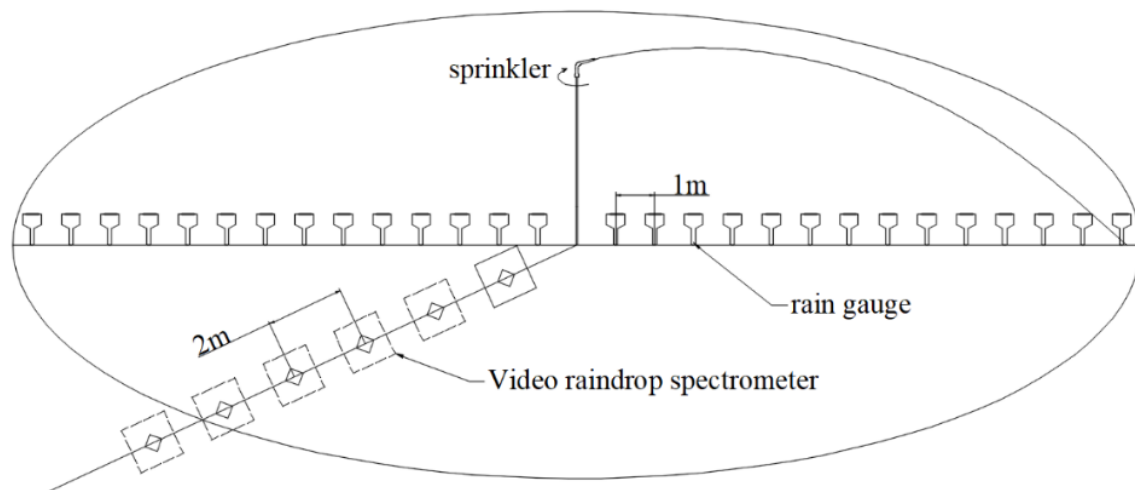


Figure 5. Schematic layout of the experimental system.



Figure 6. The test site.

2.4. Data Processing

2.4.1. Coefficient of Variation

The coefficient of variation (CV) is the ratio of the standard deviation of the water depth in each rainfall gauge to the arithmetic mean deviation [30]. The worse the uniformity of the radial water application profile of the sprinkler, the greater the measured CV. The relationship of the coefficient of variation CV is given as follows:

$$CV = \frac{SD}{MN} \times 100\%, \quad (1)$$

where CV is the coefficient of variation (%), SD is the standard deviation of the water depth received by all rain gauges (mm), and MN is the arithmetic mean of the water in all rain drums.

2.4.2. Kinetic Energy of Droplets per Unit Volume

The kinetic energy of droplets per unit volume refers to the ratio of the sum of the kinetic energy of individual droplets at different measuring points to the total volume [31]; the relationship is as follows:

$$E_{ks} = \frac{\sum_{j=1}^m E_{sdj}}{1000 \sum_{j=1}^m \frac{1}{6} \pi \bullet m_j \bullet d_j^3}, \quad (2)$$

$$E_{sd} = \frac{\sum_{i=1}^n \frac{1}{12} \pi \bullet \rho_w \bullet d_i^3 \bullet m_{di} \bullet V_{di}^2}{\sum_{i=1}^n m_{di}}, \quad (3)$$

where d is the droplet diameter (mm), E_{ks} is the kinetic energy of water droplets per unit volume (J/L), E_{sd} is the kinetic energy of a single water droplet with diameter d (J/L), m_j is the number of particles corresponding to the velocity of water droplets with diameter d , and j is the water droplet diameter class.

2.4.3. Kinetic Energy Intensity

The kinetic energy intensity represents the magnitude of the kinetic energy at the measured point per unit time. It can be determined by the water droplet diameter, droplet velocity, and water application rate [31], and the relationship is as follows:

$$K = \frac{\sum_{j=1}^m E_{sdj}}{1000 \sum_{j=1}^m \frac{1}{6} \pi \bullet d_j^3} \times \frac{h_j}{3600}, \quad (4)$$

where K is the spray kinetic energy intensity at the distance j from the nozzle (W/m^2), and h_j is the water application rate at different distances from the nozzle (mm/h).

For an overlapping sprinkler irrigation system, the uniformity coefficient of kinetic energy intensity distribution can be calculated by the Christensen average, which can reflect the distribution of rainfall energy in a sprinkler irrigation system. Therefore, the uniform coefficient of kinetic energy intensity distribution can comprehensively evaluate the advantages and disadvantages of different systems in terms of potential runoff. The equation is:

$$CU_K = \left(1 - \frac{\sum_{k=1}^N (K_k - \bar{K})}{\sum_{k=1}^N K_k} \right) \times 100\%, \quad (5)$$

where CU_k is the uniformity coefficient of the kinetic energy intensity (%), N is the total number of measuring points, and \bar{K} is the average kinetic energy intensity (W/m^2).

3. Results and Analysis

3.1. Water Discrete Degree Analysis

In order to study the difference in hydraulic performance between the non-circular nozzle and circular nozzle under low pressure and the performance of the non-circular nozzle under medium pressure, the test pressure of the circular nozzle was set to 100–200 kpa

and that of the non-circular nozzle was set to 100~300 kPa. Table 3 shows the CV for nozzles with different shapes under different working pressure levels. According to Table 3, under the same working pressure, the CV of the circular nozzle was the largest, while that of the diamond nozzle was the smallest. It indicated that the water distribution of the diamond nozzle was the most uniform, while that of the round nozzle was the least uniform. The CV of the C2 nozzle decreased with pressure; the CV of the D2 and E1 nozzles increased at first and then decreased, reaching a maximum at 150 kPa, decreasing at 250 kPa, and increasing at 300 kPa. Within the pressure range of 100–200 kPa, the CVs of both the D2 and E1 nozzles were far smaller than that of the C2 nozzle, indicating that the water distribution of the non-circular nozzles at low pressure was more uniform than that of the circular nozzles.

Table 3. Coefficient of variation for nozzles with different shapes under different working pressure levels.

Nozzle Shape (Outlet Diameter 5 mm, Inlet Cone Angle 45°)	Working Pressure (kPa)				
	100	150	200	250	300
Circle C2	1.11	0.79	0.59	/	/
Diamond D2	0.30	0.37	0.36	0.34	0.35
Ellipse E1	0.40	0.47	0.44	0.26	0.37

Table 4 displays the CV for diamond nozzles with different L/D s. According to Table 4, the CV of the D2 nozzle ($L/D = 1.32$) was the lowest, indicating that the water distribution under this L/D was the most uniform. The CV of the D1 and D3 nozzles exhibited a decreasing trend. Their maximum value appeared at 100 kPa, far exceeding that of the D2 nozzle, and the water distribution was uneven. Therefore, the diamond nozzle should be designed with an L/D of 1.32. Table 5 presents the CV for elliptical nozzles with different L/D s. According to Table 5, the CV followed the $E2 > E3 > E1$ sequence, and the E1 nozzle with the smallest L/D had the best water distribution uniformity.

Table 4. Coefficient of variation for diamond nozzles with different L/D s.

Nozzle Number	Working Pressure (kPa)				
	100	150	200	250	300
D1 ($L/D = 1.54$)	0.82	0.54	0.46	0.37	0.36
D2 ($L/D = 1.32$)	0.30	0.37	0.36	0.34	0.35
D3 ($L/D = 1.11$)	0.68	0.49	0.43	/	/

Table 5. Coefficient of variation for elliptical nozzles with different L/D s.

Nozzle Number	Working Pressure (kPa)				
	100	150	200	250	300
E1 ($L/D = 1.43$)	0.40	0.47	0.44	0.26	0.37
E2 ($L/D = 2.00$)	0.76	0.50	0.58	0.48	0.43
E3 ($L/D = 2.58$)	0.55	0.47	0.48	0.43	0.42

According to Tables 3–5, the maximum CV appeared at the low pressures of 100 kPa and 150 kPa, indicating that, at low pressure, the water distribution is more uneven. When the pressure reached 300 kPa, the CVs of all nozzles had little differences. Under low pressure, the water distribution of the non-circular nozzles (i.e., diamond and elliptical) was more uniform than that of the circular nozzle. In order to further verify the uniformity of the low-pressure water distribution of the non-circular nozzles, the radial water distribution of a single nozzle under different working pressures was investigated.

3.2. Radial Water Application Profiles

Figure 7 shows the radial water distribution curves of three nozzles (C2, D2, and E1) with an outlet diameter of 5 mm. It can be observed that the water distribution of the different nozzles was concentrated at the middle and distal end of the wetted radius, and the water application rate dropped rapidly to 0 after the peak application rate was reached. Moreover, with the increase of working pressure, the wetted radius increased, the peak application rate value decreased, and the distance from the nozzle corresponding to the peak application rate value increased. In general, the lower the working pressure, the more uneven the water distribution. Under the same working pressure, the wetted radius of the elliptical nozzle was the shortest, while that of the circular nozzle was the longest. The peak application rate was obtained in the following order: diamond < elliptical < circular. According to Figure 7 and Table 3 above, under the same working pressure, the water distribution of the diamond nozzle was the most uniform, while that of the circular nozzle was the least uniform.

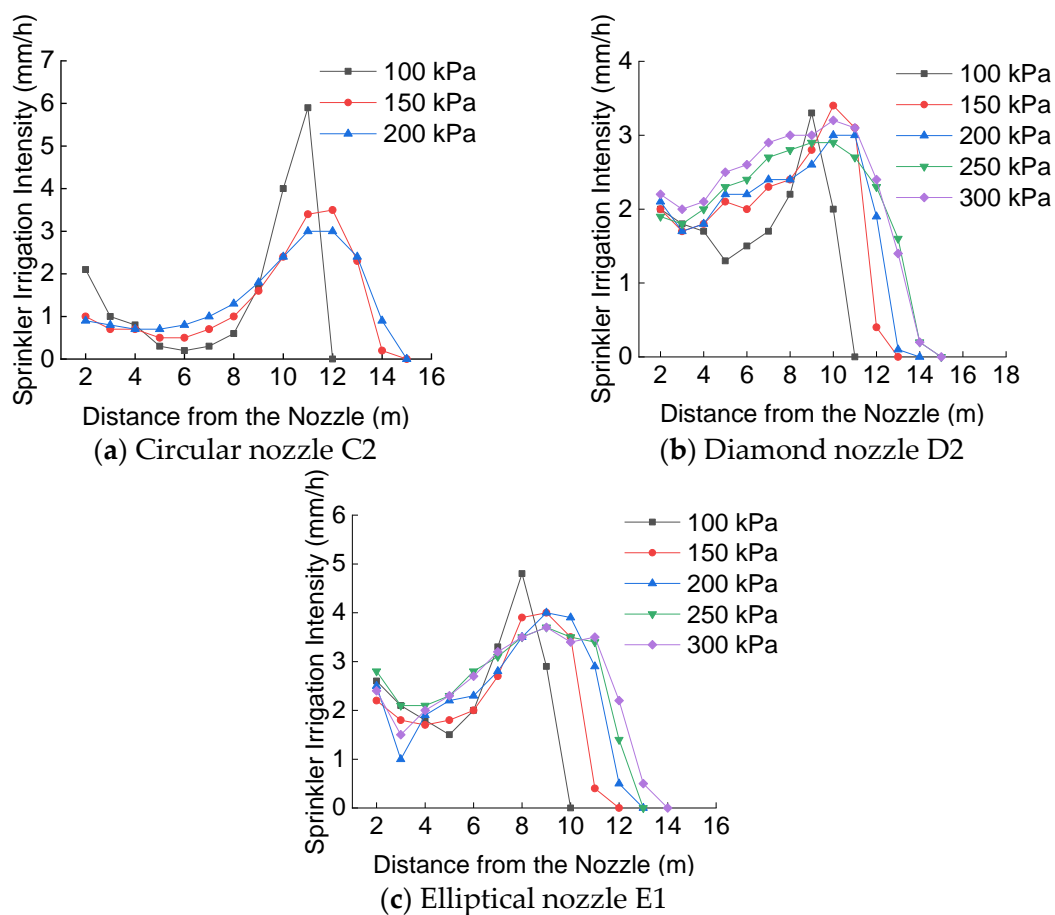


Figure 7. Radial water distribution of different nozzles under different working pressures. (C2 refers to the circular nozzle with a diameter of 5 mm; D2 refers to the diamond nozzle with an aspect ratio of 1.32; E2 refers to the elliptic nozzle with an aspect ratio of 2).

Figure 8 shows the radial water distribution of diamond nozzles D1, D2, and D3 with different outlet diameters and L/D s in the order of $D1 > D2 > D3$ under different working pressure levels. It can be observed that the wetted radius increased with decreasing L/D . Furthermore, the water application rate at the measuring point 2 m away from the sprinkler increased gradually with decreasing L/D . The amount of water was mainly concentrated at 8~12 m. The radial distribution of the water application rate exhibited an overall trend of increasing first and then decreasing. After the peak value was reached, it quickly decayed to

0. The higher the working pressure, the stronger the phenomenon that the water application rate decreased with increasing L/D .

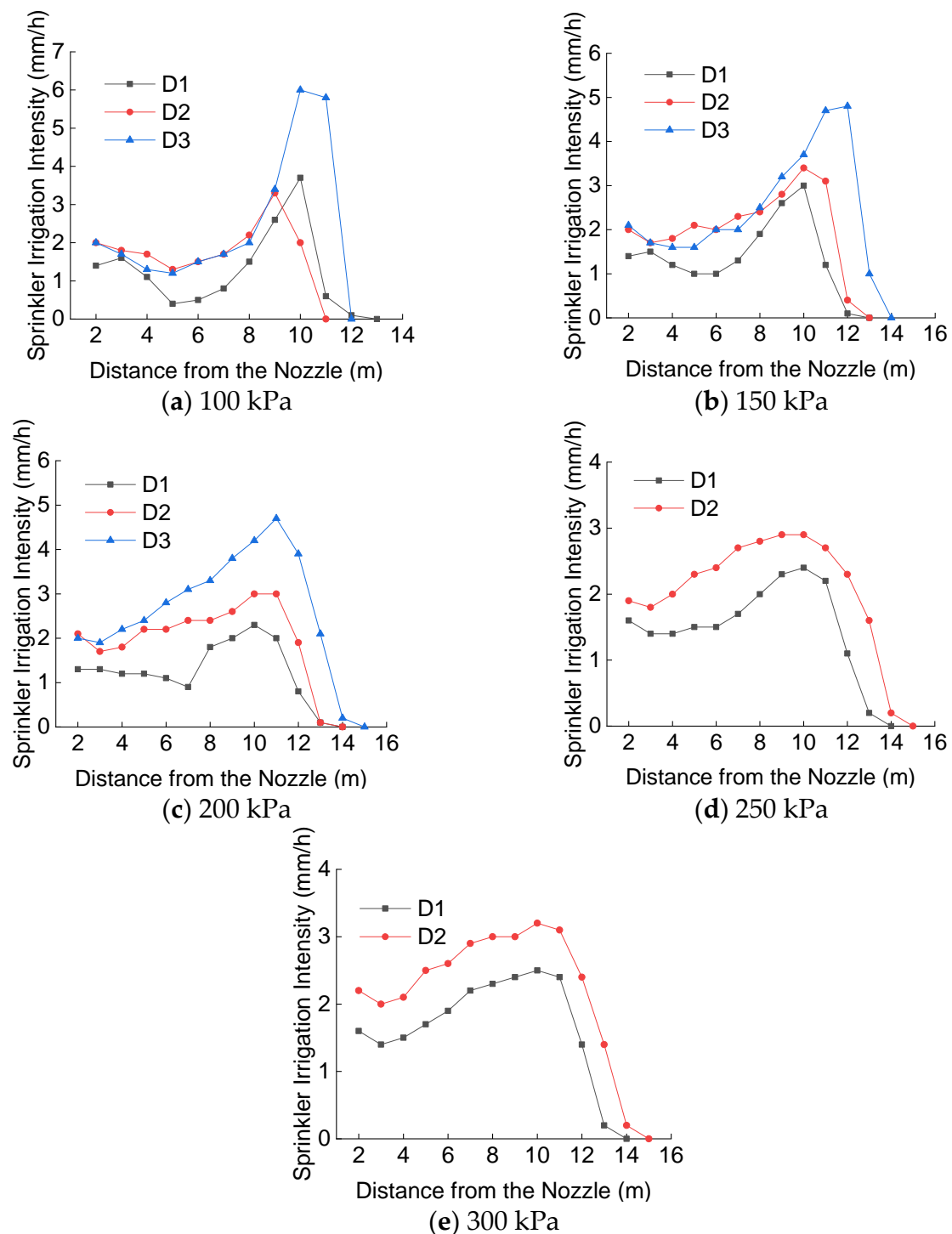


Figure 8. Radial water distribution of diamond nozzles with different outlet diameters under different working pressure levels. (D1, D2, and D3 refer to the diamond nozzles with aspect ratios of 1.54, 1.32, and 1.11, respectively).

Figure 9 shows the radial water distribution of equal flow elliptical nozzles (E1, E2, and E3) with different aspect ratios under different pressure levels. Combined with Table 5, it can be found that the E1 nozzle with the smallest L/D had the most uniform water distribution, while the E3 nozzle with the largest L/D and a slit-like shape had the largest

peak water application rate and the smallest wetted radius. In general, the smaller the aspect ratio, the closer its shape to a circle, the smaller the peak application rate value, and the more uniform the water distribution. The sprinkler water application rate of the E3 nozzle with the largest L/D was much higher than that of the other two nozzles before reaching the peak application rate, and it declined faster, soon after reaching the peak application rate. The wetted radius decreased with increasing L/D and decreasing working pressure. At 150~300 kPa, the distances from the initial position of the E1, E2, and E3 nozzles when they reached the peak application rate were 9 m, 10 m, and 8 m, respectively. This is because when the L/D was too large, the nozzle shape tended to be a “slit” and the wetted radius decreased.

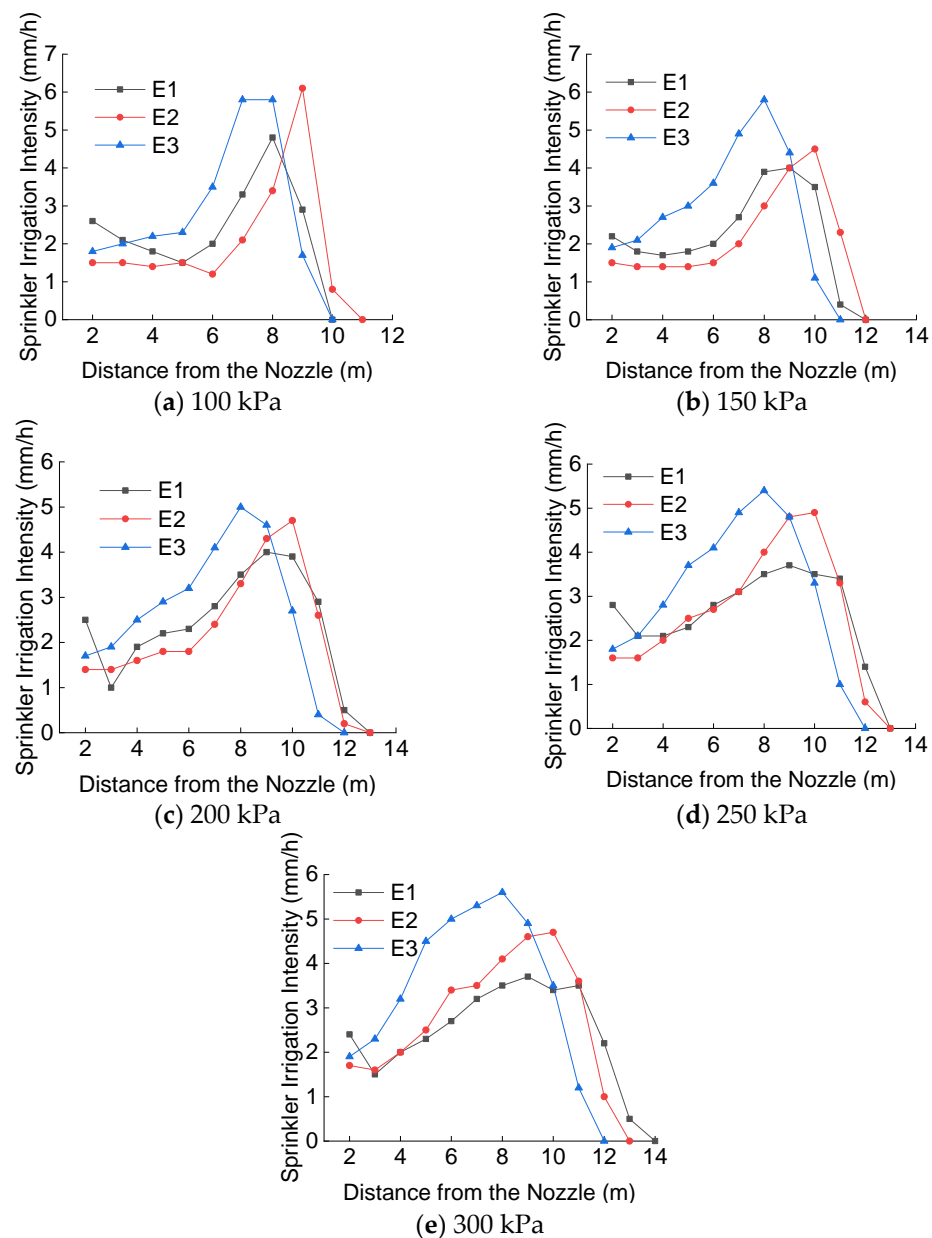


Figure 9. Radial water distribution of elliptical nozzles with different aspect ratios under different working pressure levels. (E1, E2, and E3 refer to the elliptic nozzles with aspect ratios of 1.43, 2, and 2.58, respectively).

3.3. Water Distribution Uniformity Coefficient for Combined Sprinkler Irrigation

After having determined the water distribution of the different single sprinkler heads, the main reasons affecting the uniformity of combined sprinklers are the combination mode of sprinkler heads and the combination spacing. The MATLAB software was employed to simulate and calculate the combination uniformity (*CU*) coefficients of each non-circular nozzle under different spacing in a rectangular combination arrangement at low pressure (100~200 kPa), and verify the effect of non-circular nozzles on *CU*. To avoid missing areas of water application, the combination spacing was selected as 1.0 R, 1.1 R, 1.2 R, and 1.3 R, where R is the effective spraying radius of the wetted radius of the sprinkler. The *CU* coefficients of the different nozzles under different working pressures and combination spacing are listed in Table 6.

Table 6. Combination uniformity coefficients of each nozzle under different pressures and combination spacing.

Shape	Number	Pressure (kPa)	1.0 R	1.1 R	1.2 R	1.3 R	1.4 R
Circle	C2	100	54.55	37.87	25.76	29.37	19.61
		150	58.59	58.25	50.11	37.32	26.49
		200	65.26	61.75	56.92	46.71	36.15
Diamond	D1	100	47.34	45.92	27.04	20.42	27.61
		150	63.17	59.24	47.61	45.23	46.36
		200	67.43	64.32	56.31	51.70	53.51
Diamond	D2	100	68.47	60.32	65.95	54.83	47.44
		150	69.56	70.84	63.44	55.59	54.77
		200	71.89	72.28	66.68	63.15	62.21
Diamond	D3	100	66.64	52.13	46.88	46.12	33.98
		150	66.19	62.70	60.19	48.71	41.50
		200	69.26	68.37	62.37	59.29	59.84
Ellipse	E1	100	67.92	60.02	61.47	43.52	38.02
		150	66.62	64.65	63.00	53.30	45.88
		200	68.43	65.36	58.76	53.86	54.38
Ellipse	E2	100	56.98	44.87	49.03	37.15	26.24
		150	66.05	57.09	62.24	50.34	38.82
		200	64.27	59.30	49.05	46.60	45.33
Ellipse	E3	100	62.46	62.12	52.83	38.58	43.59
		150	66.04	67.15	60.13	51.79	52.57
		200	68.51	68.72	60.87	59.05	56.46

It can be seen in Table 6 that, for the same nozzle, the *CU* coefficient increased with increasing working pressure and decreased with increasing combination spacing. Among the three different-shaped nozzles, the best combination spacing for the C2 nozzle was 1.0 R, and the *CU* coefficient was the highest (65.26%) when the working pressure was 200 kPa and the combination spacing was 1.0 R. The highest uniformity coefficient (72.28%) was presented by the D2 nozzle, under a working pressure of 200 kPa and combination spacing of 1.1 R. The highest uniformity coefficient (68.72%) of the elliptical nozzle combination was presented by the E3 nozzle, under a working pressure of 200 kPa and a combination spacing of 1.1 R. The C2 nozzle could achieve 65% uniformity at 200 kPa and 1.0 R, while the non-circular nozzles could meet the requirements at 100 kPa, indicating that the combined sprinkler irrigation with non-circular nozzles is more uniform under low pressure. The three-dimensional (3D) distribution diagrams when the *CU* coefficient of each nozzle combination was the best are presented in Figure 10.

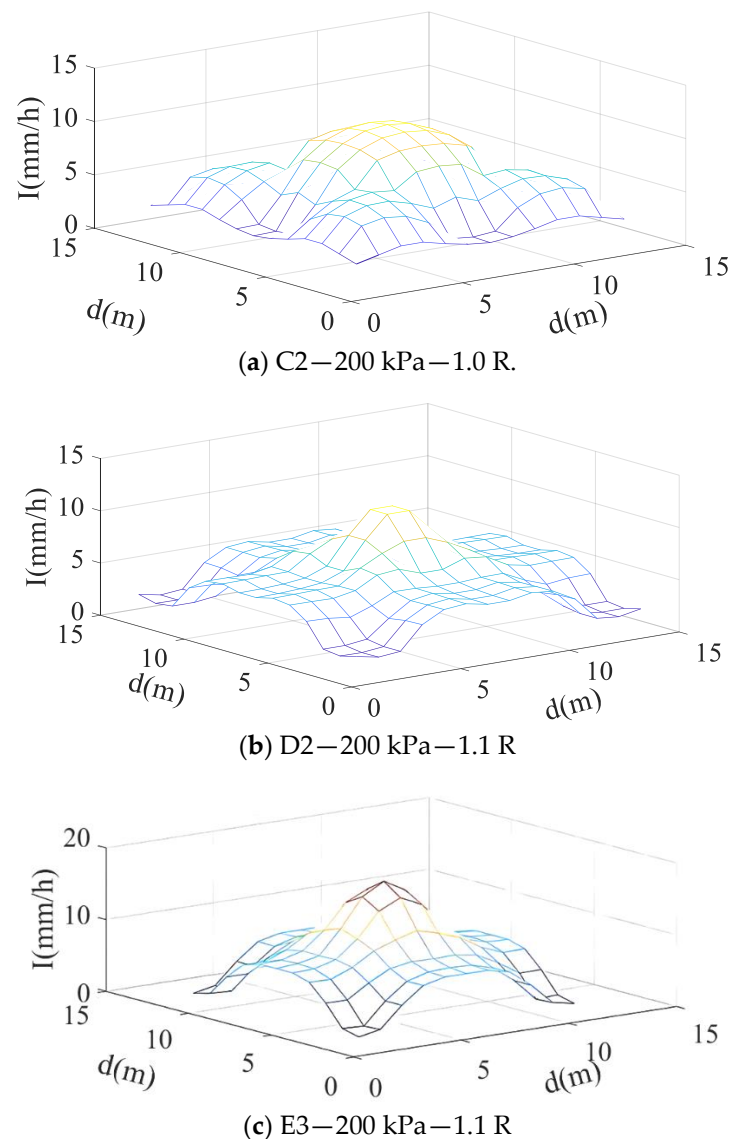


Figure 10. 3D water distribution under combined sprinkler irrigation. (C2 refers to the circular nozzle with a diameter of 5 mm; D2 refers to the diamond nozzle with an aspect ratio of 1.32; E3 refers to the elliptical nozzle with an aspect ratio of 2.58).

3.4. Kinetic Energy Intensity Distribution of Single Nozzles

Figure 11 displays the kinetic energy intensity distribution of each nozzle under different working pressure levels using B-spline curves. According to Figure 11a, the maximum kinetic energy intensity of the C2 nozzle at 100 kPa, 150 kPa, and 200 kPa was at a distance of 11 m, 12 m, and 12 m, respectively. According to Figure 11b, the maximum kinetic energy intensity of the D2 nozzle at 100 kPa, 150 kPa, 200 kPa, 250 kPa, and 300 kPa was in all cases found at a distance of 10 m. According to Figure 11c, the maximum kinetic energy intensity of the E1 nozzle at 100 kPa, 150 kPa, 200 kPa, 250 kPa, and 300 kPa was at a distance of 8 m, 10 m, 10 m, 10 m, and 10 m, respectively.

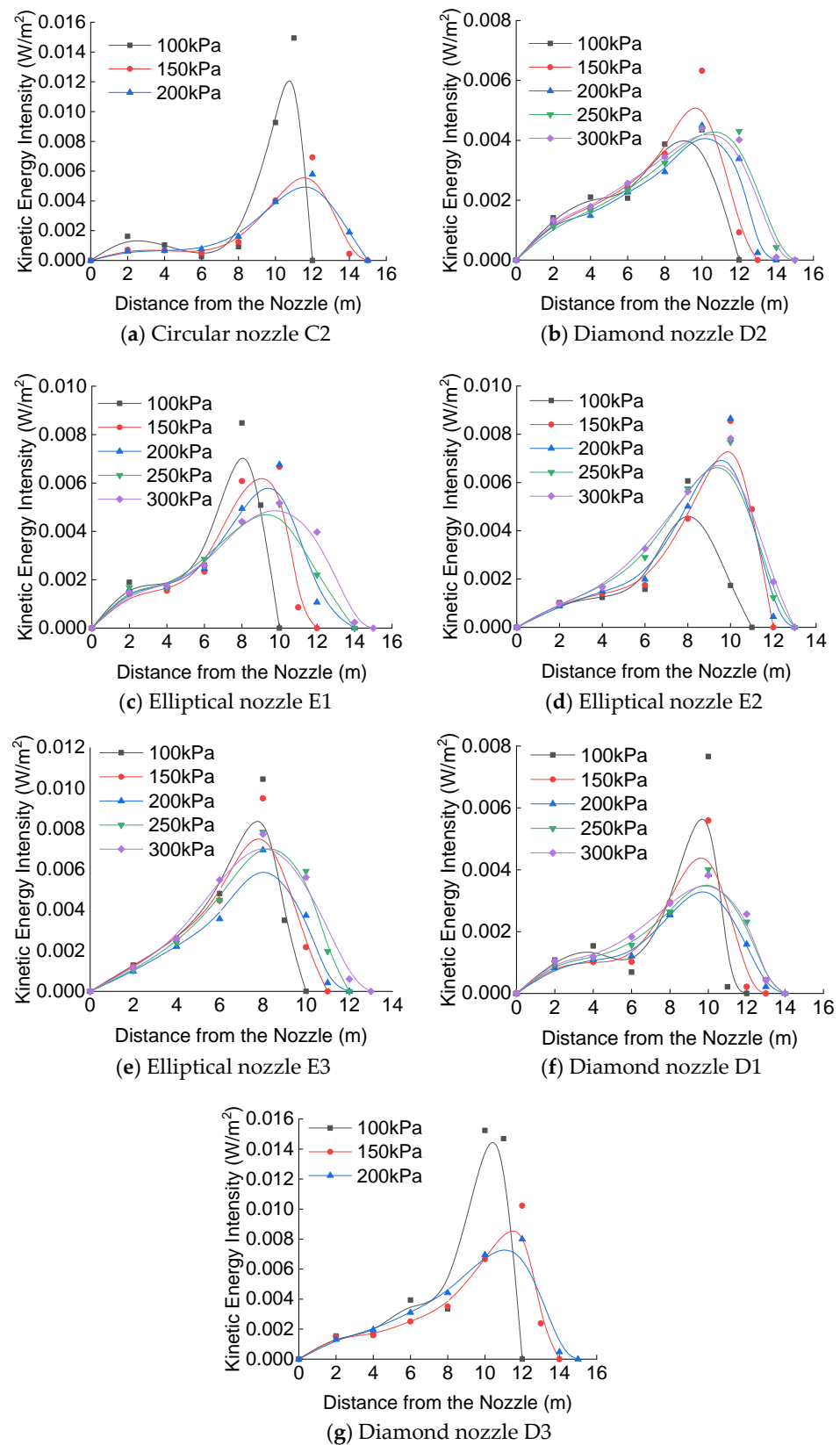


Figure 11. Kinetic energy intensity of the different single nozzles as a function of the distance from the nozzle under different working pressure levels. (C2 refers to the circular nozzle with a diameter of 5 mm; D1, D2, and D3 refer to the diamond nozzles with aspect ratios of 1.54, 1.32, and 1.11, respectively; E1, E2, and E3 refer to the elliptical nozzles with aspect ratios of 1.43, 2, and 2.58, respectively).

Based on Figure 11a–c, it can be seen that, within 0–8 m, the slope of the radial profile of the diamond nozzle was the largest, and that of the circular nozzle was the smallest. That is, the further the nozzle shape from a circle, the larger the radial increase of the kinetic energy intensity. In Figure 11c–e, it can be observed that, with the increase of the L/D , the peak value of kinetic energy intensity increased, and the distance from the nozzle position to the peak value position under each pressure was shorter. Within 0–6 m, the E3 nozzle (largest L/D) was closest to a straight line, and the slope of the radial profile was the largest, while the E1 nozzle (smallest L/D) had the smallest slope of the radial profile. This indicated that the larger the L/D , the greater the radial increase of the kinetic energy intensity. According to Figure 11b,f,g, the larger the outlet diameter, the higher the peak value of the kinetic energy intensity. Under each working pressure, the slopes of the kinetic energy intensity curves of the nozzles with an outlet diameter of 5 mm were the closest before and after reaching the peak value.

In the kinetic energy intensity curves of each nozzle plotted by B-splines, it can be observed that the peak value of the kinetic energy intensity corresponded to a distance from the nozzle position that increased with increasing working pressure, which ranged between 100 and 200 kPa. The distribution trend of the kinetic energy intensity of each nozzle along the radial direction under each working pressure was the same. It increased first and then decreased with increasing distance from the nozzle position, and then decreased rapidly to 0 after reaching the peak value of kinetic energy intensity. At 100 kPa and 150 kPa, the kinetic energy near the end of the wetted radius increased sharply, resulting in a high impact intensity on the soil surface structure, which can cause soil compaction and surface runoff.

3.5. Droplet Diameter Distribution

3.5.1. Radial Distribution of Droplet Diameter under Different Pressures

The commonly used methods for calculating the droplet diameter at home and abroad include the number-weighted method, the water-weighted average method, and the median diameter method [31,32]. In this study, the water-weighted average method was used to calculate the average droplet diameter at each measuring point. The Exp2PMod1 exponential fitting model was used, and its equation is as follows:

$$d = ae^{bl}, \quad (6)$$

where a and b are fitting coefficients, d is the droplet diameter, and l is the distance from the nozzle position.

After fitting the measured data, it was found that the fitting correlation coefficient R^2 of each nozzle shape under each working pressure was between [0.92, 0.99], which was larger than 0.9, indicating that the fitting accuracy of this exponential function was high. The results for each nozzle are presented in Figure 12. As it can be observed in Figure 12, in all cases, the higher the pressure, the smaller the slope of the exponential function curve and the smaller the average droplet diameter at the same measuring point. This indicated that the increasing trend of the droplet diameter along the distance from the nozzle decreased with increasing pressure and the jet break-up was more severe. Among them, the slope of the radial profile of the C2 nozzle decreased the most. As shown in Table 5, among these three nozzles under the same pressure, the slope of the radial profile of the diamond nozzle was the largest and that of the circular nozzle was the smallest. It indicated that the droplet diameter of the diamond nozzle increased the most along the distance from the nozzle position.

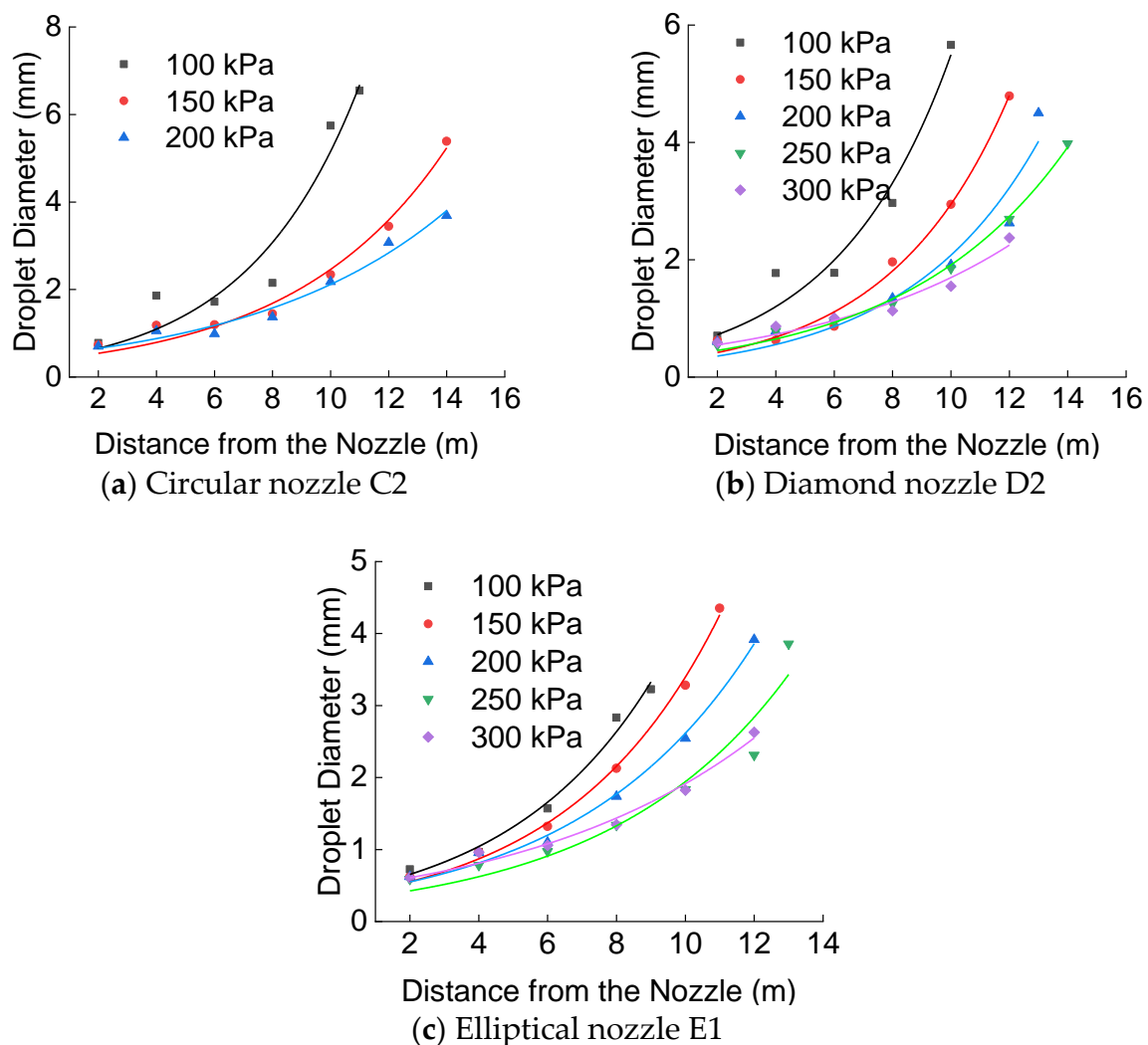


Figure 12. Relationship between average droplet diameter and distance from the nozzle. (C2 refers to the circular nozzle with a diameter of 5 mm; D2 refers to the diamond nozzle with an aspect ratio of 1.32; E1 refers to the elliptic nozzle with an aspect ratio of 1.43).

In addition, when the droplet diameter was 3 mm, the distance from the C2 nozzle at 100 kPa, 150 kPa, and 200 kPa was 7.9 m, 11 m, and 12.4 m, respectively; the distance from the D2 nozzle at 100 kPa, 150 kPa, 200 kPa, and 250 kPa was 7.6 m, 10 m, 11.7 m, and 12.5 m, respectively; and the distance from the E1 nozzle at 100 kPa, 150 kPa, 200 kPa, and 250 kPa was 8.5 m, 9.5 m, 10.7 m, and 12.3 m, respectively. At 300 kPa, the droplet diameters of the diamond and elliptical nozzles were less than 3 mm. In general, droplets with a smaller diameter tend to drift and have evaporation losses, while larger-diameter droplets can cause greater damage to the soil surface, which is not conducive to water and soil conservation and crop growth. Thus, the droplet diameter range suitable for spraying is within 1~3 mm [15]. Consequently, the E1 nozzle had the optimal wetted radius except for the 100 kPa case, where the C2 nozzle had the optimal wetted radius. When the distance was larger than 8 m, the pressure had a significant effect on droplet diameter.

3.5.2. Radial Distribution of Droplet Diameter under Different Aspect Ratios

Figure 13 depicts the relationship between mean droplet diameter and distance from the nozzle for different L/D s at different working pressure levels. For the nozzles with the same L/D , the slope of the exponential curve of the droplet diameter decreased with increasing pressure, i.e., the radial increase trend of the droplet diameter decreases with increasing pressure. Under the same pressure, shape, inlet cone angle, outlet diameter, and

different aspect ratios, the droplet diameter at each measuring point was almost the same within 6 m from the nozzle position. The relationship between average droplet diameter distance from the nozzle generally followed the following order of $E3 > E2 > E1$, i.e., the larger the L/D , the larger the average droplet diameter. The E3 nozzle (largest L/D) had the shortest wetted radius and the largest overall droplet diameter. The E1 nozzle (smallest L/D) had the smallest droplet diameter along the radial direction and a relatively large wetted radius. Therefore, nozzles with a small L/D should be selected in sprinkler spraying.

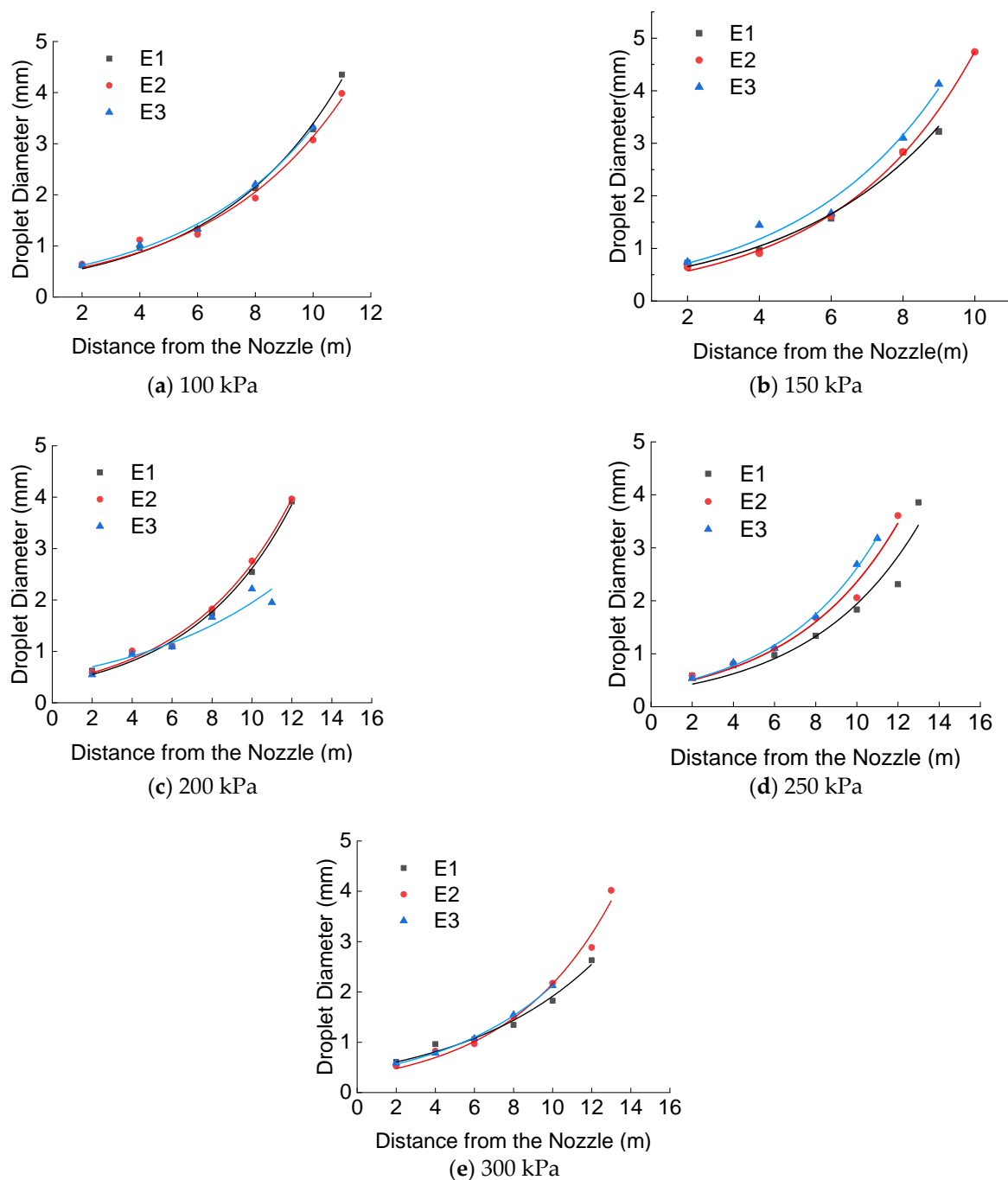


Figure 13. Relationship between mean droplet diameter and distance from the nozzle for different aspect ratios at different working pressure levels. (E1, E2, and E3 refer to the elliptical nozzles with aspect ratios of 1.43, 2, and 2.58, respectively).

3.6. Droplet Velocity Distribution

3.6.1. Droplet Velocity Distribution of Nozzles with Different Shapes

The velocity of spraying droplets is an important factor to determine the kinetic energy of striking droplets. 2DVD was used to measure the velocity of droplets with different diameters sprayed from different nozzles.

There is a logarithmic function that can express the relationship between droplet diameter and droplet velocity. The relationship is as follows [18]:

$$v = a - b \ln(d + c)a, \quad (7)$$

where a , b , and c are fitting coefficients, v is the droplet velocity, and d is the droplet diameter.

Figure 14 shows the results where the fitting correlation coefficient R^2 was between [0.93, 0.97]. As it can be observed, for the nozzles with the same inlet cone angle and outlet diameter, the velocity curve slope of the circular nozzle was the largest and that of the elliptical nozzle was the smallest, i.e., with the increase of the droplet diameter, the increase rate of the velocity of the elliptical nozzle droplets was the smallest. The droplet velocity increased with increasing droplet diameter, and the increasing trend gradually decreased, indicating that droplet diameter is an important factor affecting droplet velocity. In general, the fitted curves of the three nozzles with equal flow rate were almost identical. It shows that, when the flow rate, inlet cone angle, and outlet diameter are the same, the nozzle outlet shape has little effect on the relationship between average droplet diameter and droplet velocity.

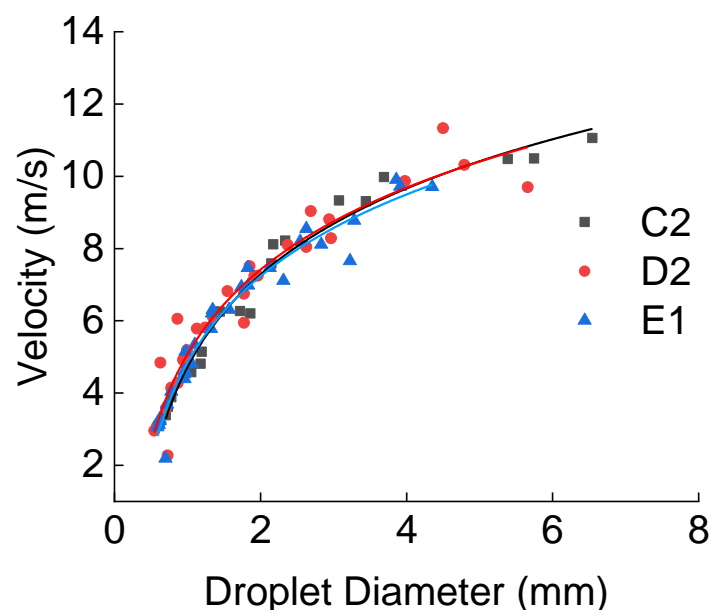


Figure 14. Relationship between average droplet diameter and velocity sprayed from nozzles with different shapes. (C2 refers to the circular nozzle with a diameter of 5 mm; D2 refers to the diamond nozzle with an aspect ratio of 1.32; E1 refers to the elliptical nozzle with an aspect ratio of 1.43).

3.6.2. Droplet Velocity Distribution under Different Aspect Ratios

The relationship between the diameter and velocity of droplets sprayed from elliptical nozzles with different aspect ratios is shown in Figure 15. The fitting correlation coefficient R^2 was between [0.86, 0.98]. As it can be observed in Figure 15, for elliptical nozzles with the same inlet cone angle and outlet diameter, and different aspect ratios, the velocity curve slope followed the following order: $E3 > E2 > E1$, i.e., the velocity curve slope increased with increasing L/D . In addition, the magnitude of droplet velocity increased with increasing droplet diameter. At the same droplet diameter, the droplet velocity of the E2 nozzle

was always the maximum. When the droplet diameter was less than 2.5 mm, the droplet velocity of the elliptical nozzle followed the $E1 > E3$ order. When the droplet diameter was greater than 2.5 mm, the droplet velocity followed the opposite order ($E3 > E1$). This indicated that there was an aspect ratio between the maximum and minimum aspect ratios. At this aspect ratio, the velocity of droplets with the same diameter was the highest, and therefore, the kinetic energy of the striking droplets was the highest.

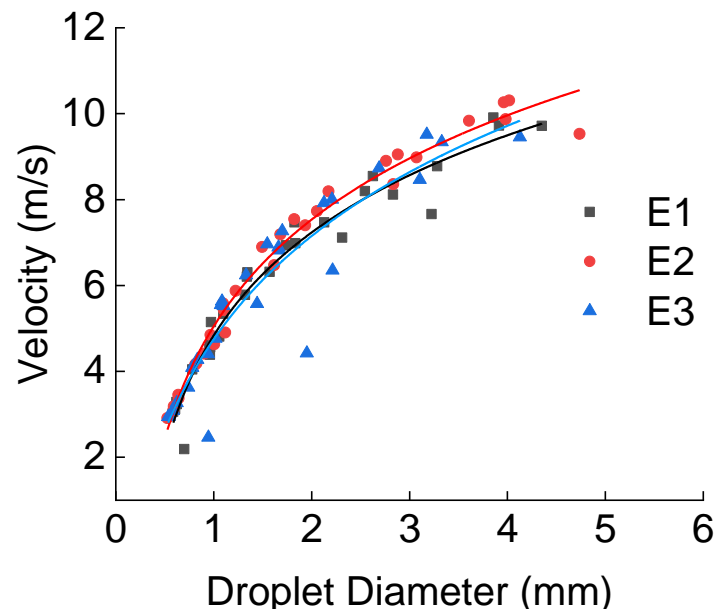


Figure 15. Relationship between average droplet diameter and velocity sprayed from elliptical nozzles with different aspect ratios. (E1, E2, and E3 refer to the elliptic nozzles with aspect ratios of 1.43, 2, and 2.58, respectively).

The relationship between the diameter and velocity of droplets sprayed from diamond nozzles with different aspect ratios is demonstrated in Figure 16. The fitting correlation coefficient R^2 was between [0.93, 0.96]. As it can be seen in Figure 16, for nozzles with the same shape and inlet cone angle, the velocity curve slope followed the following order: $D3 > D2 > D1$, i.e., the velocity curve slope decreased with increasing L/D . In general, the smaller the L/D , the higher the droplet velocity, which increased with increasing droplet diameter. When the droplet diameter was less than 5 mm, the $D1 > D2 > D3$ order was followed, indicating that, when the droplet diameter is the same, the smaller the L/D , the lower the droplet velocity.

3.7. Kinetic Energy per Unit Volume Radial Profiles

Based on the kinetic energy distribution trend of droplets per unit volume, the kinetic energy per unit volume at different measuring points was calculated. Figure 17 shows the radial distribution of kinetic energy per unit volume of droplets sprayed from different nozzles under different pressure levels. As it can be seen in Figure 17, the higher the working pressure, the lower the kinetic energy per unit volume of the droplets at the same position, the smaller the increase of kinetic energy, and the less the damage to crops and soil surface. At 2 m, the kinetic energy per unit volume of droplets from each nozzle was not significantly different under all working pressures. According to Figure 17a–c, the maximum kinetic energy per unit volume of the elliptical nozzle was the lowest among the nozzles with equal flow and the same inlet cone angle and outlet diameter under each working pressure. At 100 kPa, the maximum kinetic energy per unit volume of the circular nozzle was the highest. According to Figure 17c–e, the larger the L/D , the smaller the wetted radius. The maximum kinetic energy per unit volume of the E1 nozzle (smallest

L/D) at 100 kPa was the lowest. At 150–300 kPa, the E3 nozzle (largest L/D) had the lowest kinetic energy per unit volume. In Figure 17b,f,g, it can be observed that, the smaller the outlet diameter, the lower the kinetic energy per unit volume.

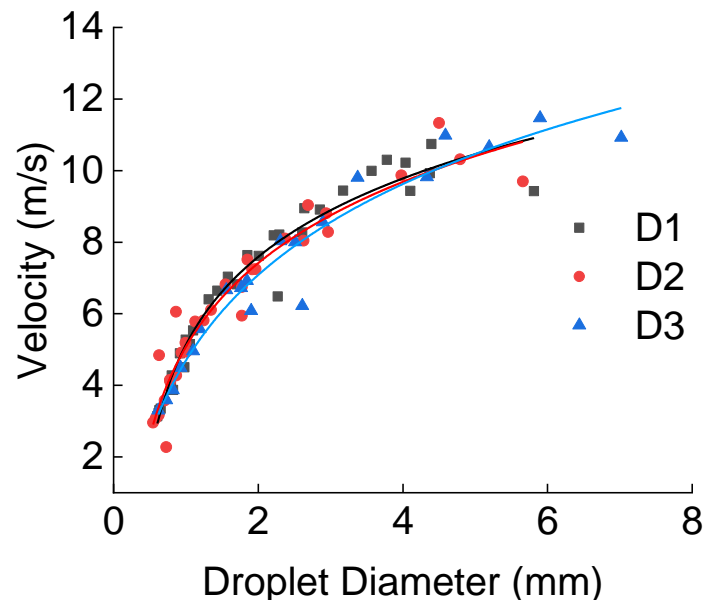


Figure 16. Relationship between droplet velocity and diameter sprayed from diamond nozzles with different aspect ratios. (D1, D2, and D3 refer to the diamond nozzles with aspect ratios of 1.54, 1.32, and 1.11, respectively).

In order to further investigate the radial distribution characteristics of the droplet kinetic energy per unit volume of the non-circular nozzles, in this paper, regression analysis on the kinetic energy per unit volume of each nozzle under various pressures was performed, and a distribution model of the kinetic energy based on the distance from the nozzle was established [30]. The relationship is given in the following equation:

$$E_{ks} = al + b, \quad (8)$$

where a and b are fitting coefficients, E_{ks} is the droplet kinetic energy per unit volume, and l is the distance from the nozzle position.

After fitting the measured data, it was found that the fitting correlation coefficient R^2 of the kinetic energy per unit volume for the non-circular nozzles was between [0.89, 0.99], indicating that the fitting accuracy was high.

The data of the droplet kinetic energy per unit volume of the three elliptical nozzles with different aspect ratios under different working pressures were uniformly regressed, and the kinetic energy per unit volume was further analyzed. A mathematical model of the relationship between droplet kinetic energy per unit volume E_{ks} , distance from the nozzle l , aspect ratio β , and working pressure P for non-circular nozzles was established. The functional relationship is as follows:

$$E_{ks} = 2.775P^{-0.318}l + 0.0926\beta + 0.932 \quad (R^2 = 0.924), \quad (9)$$

The fitting coefficient of the droplet kinetic energy per unit volume for the elliptical nozzles with different aspect ratios was 0.92, indicating that the fitting accuracy was high. According to this regression equation, we can obtain the influence of the change of aspect ratio on the kinetic energy of water droplets under different working pressures.

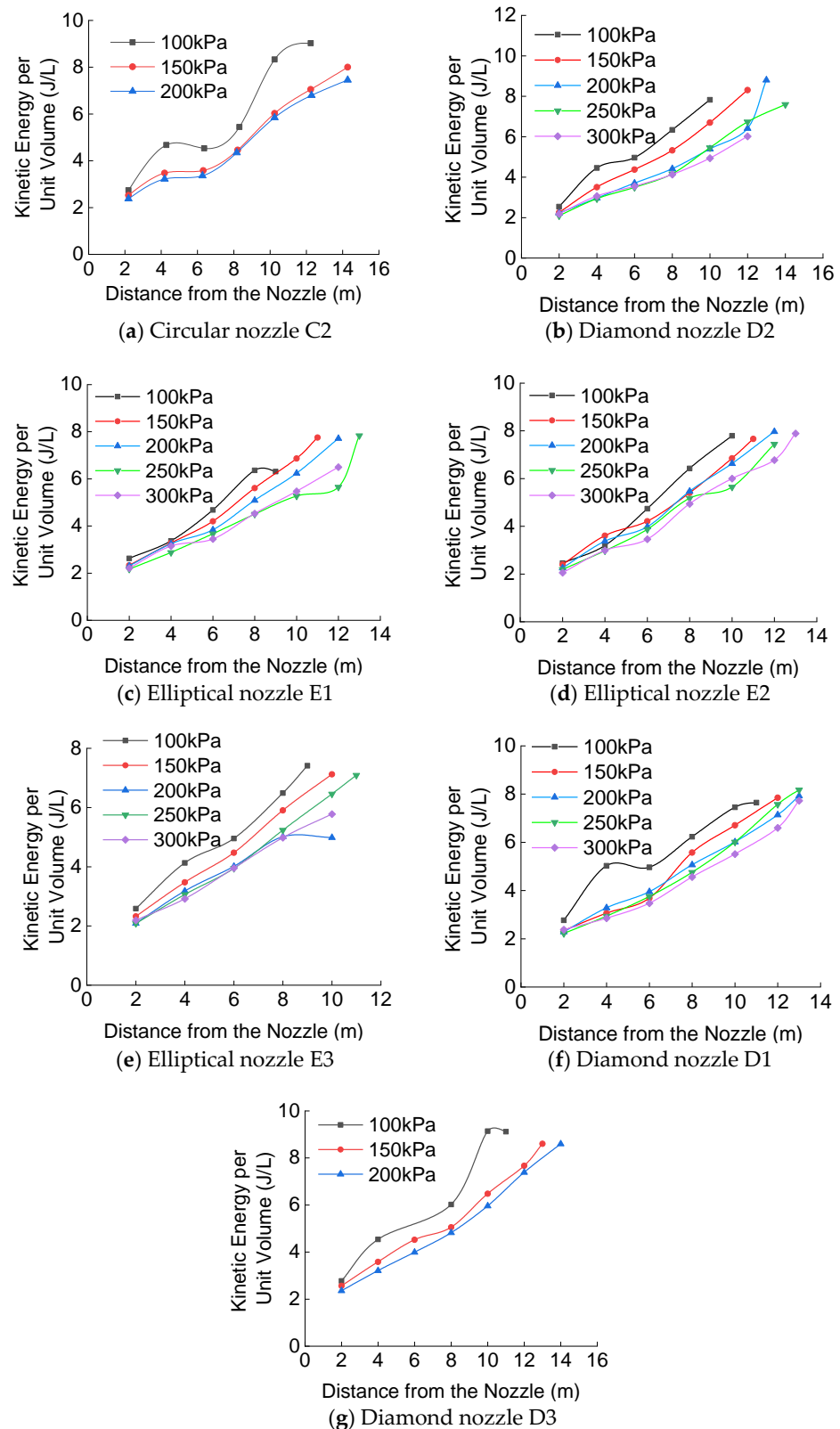


Figure 17. Kinetic energy per unit volume as a function of the distance from each nozzle under different working pressure levels. (C2 refers to the circular nozzle with a diameter of 5 mm; D1, D2, and D3 refer to the diamond nozzles with aspect ratios of 1.54, 1.32, and 1.11, respectively; E1, E2, and E3 refer to the elliptic nozzles with aspect ratios of 1.43, 2, and 2.58, respectively).

3.8. Uniformity Coefficient of Kinetic Energy Intensity Distribution of Combined Sprinkler

In general, the sprinklers in sprinkler irrigation systems are arranged in square and triangular shapes. In this study, the working pressure of the sprinkler was 100 kPa, 150 kPa, and 200 kPa, and a square arrangement was simulated. The uniformity coefficient of the kinetic energy intensity of combined sprinkler irrigation was simulated and calculated by using the MATLAB software. The combination spacing was selected as 1.0 R, 1.1 R, 1.2 R, and 1.3 R, where R is the wetted radius. The calculation results are listed in Table 7.

Table 7. Uniformity coefficient of the kinetic energy intensity distribution for each nozzle under different combination spacing.

Shape	Number	Pressure (kPa)	1.0 R	1.1 R	1.2 R	1.3 R
Circle	C2	100	40.07	29.60	18.53	18.53
		150	49.85	45.61	22.77	10.37
		200	55.93	51.15	30.90	22.51
Diamond	D1	100	49.32	42.63	11.27	11.27
		150	51.78	46.68	19.08	19.08
		200	63.52	45.24	45.48	49.98
Diamond	D2	100	63.62	67.59	67.59	40.31
		150	56.34	52.41	34.58	34.58
		200	65.36	59.13	49.19	54.15
Diamond	D3	100	52.32	53.37	53.37	18.18
		150	57.12	53.72	36.09	28.76
		200	59.39	59.51	39.88	39.60
Ellipse	E1	100	55.65	48.67	48.67	29.94
		150	57.02	49.22	32.61	32.61
		200	57.02	51.99	33.90	33.90
Ellipse	E2	100	49.20	38.37	38.37	20.99
		150	55.02	53.66	28.17	28.17
		200	51.84	45.69	21.36	21.36
Ellipse	E3	100	52.81	41.12	41.12	35.87
		150	51.82	39.31	39.31	35.47
		200	57.78	49.95	49.95	39.98

It can be observed that the uniformity coefficients of the combined kinetic energy intensity of the nozzles under the three pressure levels were different under different spacing. The results indicated that the best combination spacing for the C2 nozzle was 1.0 R, and the best kinetic energy intensity distribution uniformity coefficients at 100 kPa, 150 kPa, and 200 kPa were 40.07%, 49.85%, and 55.93%, respectively. The best kinetic energy intensity distribution coefficient among the diamond nozzles was exhibited by the D2 nozzle. When the outlet diameter was 5 mm, the working pressure was 100 kPa, and the best combination spacing was 1.1 R and 1.2 R, the optimal kinetic energy intensity distribution uniformity coefficient was 67.59%. The optimal combination spacing for the elliptical nozzles was 1.0 R. The optimal uniformity coefficient of the kinetic energy intensity distribution was exhibited by the E3 nozzle (largest L/D) at the working pressure of 100 kPa (57.78%). In addition, it was found that the uniformity coefficient of the kinetic energy intensity distribution of the combined sprinkler increased gradually with increasing pressure. The 3D distributions of the combined sprinkler irrigation kinetic energy intensity of the nozzles with the best uniformity coefficient per shape type are exhibited in Figure 18.

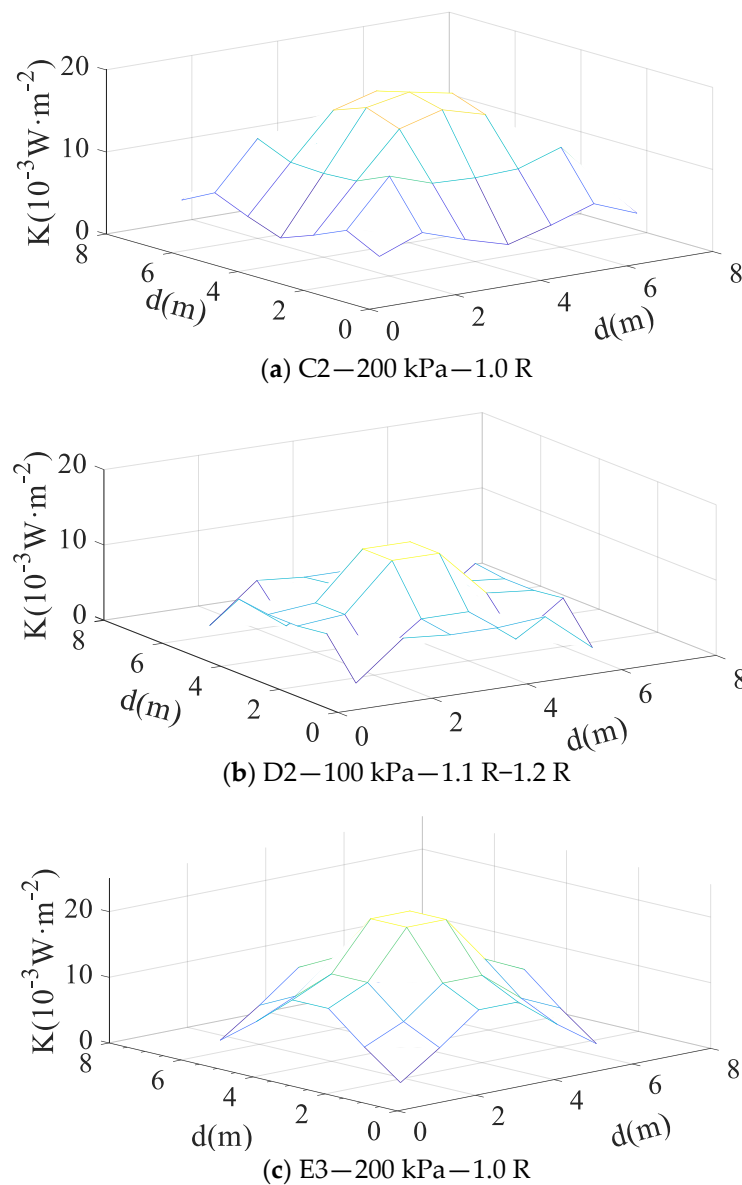


Figure 18. Distribution of kinetic energy intensity under combined sprinkler irrigation for each nozzle shape with the best uniformity coefficient. (C2 refers to the circular nozzle with a diameter of 5 mm; D2 refers to the diamond nozzle with an aspect ratio of 1.32; E3 refers to the elliptic nozzle with an aspect ratio of 2.58).

4. Discussion

Most of the research on the distribution characteristics of water droplets in non-circular nozzles focuses on the influence of the shape and pressure on the jet shape. In this study, a video raindrop spectrometer is used to supplement the research on the influence of the shape and pressure of non-circular nozzles on the distribution characteristics of water droplets, such as diameter, velocity, and kinetic energy. The diameter of water droplets increases in the radial direction and decreases with the increase of pressure. The larger the diameter of the outlet is, the greater the speed of water droplets increases with the diameter of water droplets. When the diameter of water droplets is the same, the larger the diameter of outlet, the smaller the velocity of water droplets. The impact kinetic energy per unit volume of droplets at the same position and its growth range decrease with the increase of pressure.

In addition, the influence of the aspect ratio of a non-circular nozzle on spraying hydraulic performance and water droplet distribution characteristics is studied in this paper. The shape coefficient of the non-circular nozzle increases with the increase of aspect ratio, and the range decreases with the increase of aspect ratio. Under five working pressures, the diameter of water droplets in the diamond nozzle increases the most along the radial direction. The larger the aspect ratio is, the greater the speed of water droplets increases with the diameter of water droplets. With the increase of droplet diameter, the growth rate in droplet velocity of the elliptical nozzle is the smallest, while that of circular nozzle is the largest. The nozzle with the outlet diameter of 5 mm has the smallest average droplet diameter, and the droplet diameter decreases the most along the longitudinal direction.

5. Conclusions

A prediction model which can accurately reflect the droplet diameter, velocity, and kinetic energy distribution per unit volume of three types of nozzles was developed, and a fitting function of the relationship between L/D and kinetic energy per unit volume for non-circular nozzles was established. The relationship between droplet diameter and kinetic energy and the distance from the nozzle is an exponential and a linear function, respectively, and the fitting correlation coefficients were between [0.92, 0.99] and [0.89, 0.99], respectively. The distribution of droplet velocity and diameter was found to be logarithmic, and the fitting coefficient was between [0.86 and 0.98]. The relationship between L/D and kinetic energy was linear, and the fitting coefficient was 0.924. In all cases, the fitting accuracy was high.

Among the tested nozzles, the sprinkler with the circular nozzle generated the largest CV , while the elliptical and diamond nozzles generated similar CV s. When operating at the same working pressure, the diamond nozzle exhibited the smallest peak application rate value and the largest radially increasing trend in droplet diameter, while the elliptical nozzle had the lowest maximum droplet kinetic energy per unit volume. The more the nozzle shape deviated from a circle, the larger the radial increase of the kinetic energy intensity. For elliptical nozzles with equal flow and area, the smaller the L/D , the smaller the average droplet diameter and velocity, the lower the peak sprinkler water application rate, the more uniform the water distribution, the larger the wetted radius, and the smaller the radial increase of the kinetic energy intensity. The water distribution uniformity was the best when the L/D was the smallest.

Under a working pressure of 200 kPa and a combination spacing of 1.0 R, the uniformity coefficients of combined sprinkler irrigation and combined kinetic energy intensity distribution with circular nozzles were the highest, i.e., 65.26% and 55.93%, respectively. The uniformity coefficient of combined sprinkler irrigation with diamond nozzles was the highest (72.28%) when the L/D was 1.32, the working pressure was 200 kPa, and the combination spacing was 1.1 R. The combined kinetic energy intensity distribution of the diamond nozzle was the most uniform (67.59%) when the outlet diameter was 5 mm, the working pressure was 100 kPa, and the combination spacing was 1.1 R and 1.2 R. Among the three elliptical nozzles with the same flow rate and different L/D , the one with the largest L/D had the highest uniformity coefficient (68.72%) when the working pressure was 200 kPa and the combination spacing was 1.1 R. When the combination spacing was 1.0 R, the distribution uniformity coefficient of combination kinetic energy intensity was also the highest (57.78%). In general, the larger the L/D of the nozzle, the lower the maximum droplet kinetic energy per unit volume.

Author Contributions: Conceptualization, Y.J. and H.L. (Hong Li); methodology, Y.J., Z.W. and J.L.; validation, Z.W.; formal analysis, Y.J., Z.W. and J.L.; investigation, Y.J., H.L. (Hong Li) and H.L. (Hao Li); data curation, J.L.; writing—original draft preparation, J.L.; writing—review and editing, Y.J. and Z.W.; visualization, J.L.; supervision, Y.J. and H.L. (Hao Li); project administration, Y.J. and H.L. (Hong Li). All authors have read and agreed to the published version of the manuscript.

Funding: This research was funded by the Postgraduate Research & Practice Innovation Program of Jiangsu Province, grant number SJCX22_1870, the Jiangsu Province and Education Ministry Co-sponsored Synergistic Innovation Center of Modern Agricultural Equipment, grant number XTCX2018, the Changzhou Key Research and Development Program, grant number CE20222024, Zhenjiang Key Research and Development Program, grant number CN2022003, and the Youth Talent Development Program of Jiangsu University.

Institutional Review Board Statement: Not applicable.

Data Availability Statement: The data presented in this study are available on request from the corresponding author.

Acknowledgments: Thanks for grateful to the Postgraduate Research & Practice Innovation Program of Jiangsu Province (SJCX22_1870), the Jiangsu Province and Education Ministry Co-sponsored Synergistic Innovation Center of Modern Agricultural Equipment (XTCX2018), the Changzhou Key Research and Development Program (No. CE20222024), Zhenjiang Key Research and Development Program (No. CN2022003) and the Youth Talent Development Program of Jiangsu University.

Conflicts of Interest: The authors declare no conflict of interest.

References

- Li, J. Study on the atomizing condition of non-circular nozzles. *J. Hydraul. Eng.* **1991**, *3*, 28–32+64.
- Chen, C.; Yuan, S.; Li, H.; Wang, C. Effect of Non-circle Nozzle on Hydraulic Performance of Impact Variable-rate Sprinkler. *Trans. Chin. Soc. Agric. Mach.* **2011**, *42*, 111–115.
- Bao, Y.; Liu, J.; Liu, X.; Tian, K.; Zhang, Q. Experimental study on the effects of pressure on water distribution model of low-pressure sprinkler. *J. Drain. Irrig. Mach. Eng.* **2016**, *34*, 81–85.
- Yan, H.J.; Bai, G.; He, J.Q.; Lin, G. Influence of Droplet Kinetic Energy Flux Density from Fixed Spray-Plate Sprinklers on Soil Infiltration, Runoff and Sediment Yield. *Biosyst. Eng.* **2011**, *110*, 213–221. [[CrossRef](#)]
- Shi, Y.; Zhu, X.; Hu, G.; Zhang, A.; Li, J. Influence of different working conditions on water distribution in sprinkler irrigation. *J. Drain. Irrig. Mach. Eng.* **2021**, *39*, 318–324.
- Liu, H.; Kang, Y. Effects of Droplets Kinetic Energy on Soil Infiltration Rate and Surface Runoff under Sprinkler Irrigation. *J. Irrig. Drain.* **2002**, *21*, 71–74+79. [[CrossRef](#)]
- Jiang, Y.; Li, H.; Xiang, Q.; Chen, C. Experimental study on breakup length and range of free jet of non-circle jet nozzle. *J. Irrig. Drain.* **2014**, *33*, 149–153. [[CrossRef](#)]
- William, E. Hart Sprinkler Distribution Analysis With a Digital Computer. *Trans. ASAE* **1963**, *6*, 0206–0208. [[CrossRef](#)]
- Yuan, S.; Li, H.; Wang, X. Status, problems, trends and suggestions for water-saving irrigation equipment in China. *J. Drain. Irrig. Mach. Eng.* **2015**, *33*, 78–92.
- Bubenzer, G.D.; Jones, B.A., Jr. Drop Size and Impact Velocity Effects on the Detachment of Soils Under Simulated Rainfall. *Trans. ASAE* **1971**, *14*, 0625–0628. [[CrossRef](#)]
- Mohammed, D.; Kohl, R.A. Infiltration Response to Kinetic Energy. *Trans. ASAE* **1987**, *30*, 0108–0111. [[CrossRef](#)]
- Christiansen, J.E. *Irrigation by Sprinkling*; University of California: Berkeley, CA, USA, 1942; Volume 4.
- Abd El-Wahed, M.H.; Medici, M.; Lorenzini, G. Harvesting Water in a Center Pivot Irrigation System: Evaluation of Distribution Uniformity with Varying Operating Parameters. *J. Eng. Thermophys.* **2015**, *24*, 143–151. [[CrossRef](#)]
- Li, Y.; Liu, J. Prospects for development of water-saving irrigation equipment and technology in China. *J. Drain. Irrig. Mach. Eng.* **2020**, *38*, 738–742.
- Wu, P.; Zhu, D.; Lv, H.; Zhang, L. Hydraulics problems in farmland irrigation. *J. Drain. Irrig. Mach. Eng.* **2012**, *30*, 726–732.
- Tu, Q.; Li, H.; Wang, X.; Li, Y.; Jiang, Y. Comparison and selection of small-scale irrigation machines with multiple sprinklers based on grey relational analysis. *J. Jiangsu Univ.* **2014**, *35*, 656–662.
- Xu, H.; Gong, S.; Jia, R.; Liu, X. Study on droplet size distribution of ZY sprinkler head. *J. Hydraul. Eng.* **2010**, *41*, 1416–1422. [[CrossRef](#)]
- Gong, X.; Zhu, D.; Zhang, L.; Zhang, Y.; Ge, M.; Yang, W. Drop Size Distribution of Fixed Spray-plate Sprinklers with Two-dimensional Video Disdrometer. *Trans. Chin. Soc. Agric. Mach.* **2014**, *45*, 128–133+148.
- Lorenzini, G. Water droplet dynamics and evaporation in an irrigation spray. *Trans. ASABE* **2006**, *49*, 545–549. [[CrossRef](#)]
- Ouazaa, S.; Burguete, J.; Paniagua, M.P.; Salvador, R.; Zapata, N. Simulating Water Distribution Patterns for Fixed Spray Plate Sprinkler Using the Ballistic Theory. *Span. J. Agric. Res.* **2014**, *12*, 850. [[CrossRef](#)]
- Zhu, X.; Liu, X.; Liu, J.; Yuan, S.; Bao, Y. Droplet kinetic energy distribution regulation of complete fluidic sprinkler. *Trans. Chin. Soc. Agric. Eng.* **2015**, *31*, 26–31.
- Li, J.; Ma, F. Effect of nozzle shape on the spraydrop kinetic energy from sprinklers. *J. Irrig. Drain.* **1997**, *16*, 3–8.
- Chen, D. Shape and structure of special nozzle. *Water Sav. Irrig.* **1982**, *3*, 37.
- Li, Y.; Liu, J.; Guo, Z.; Liu, X.; Lou, Y. Research and development of hydraulic performance of energy-saving special-shaped nozzle. *J. Irrig. Drain.* **1990**, *2*, 43–50. [[CrossRef](#)]

25. Wei, Y.; Yuan, S.; Li, H.; Xiang, Q.; Chen, C. Hydraulic Performance Experiment of the Variable-rate Sprinkler with Non-circle Nozzle. *Trans. Chin. Soc. Agric. Mach.* **2011**, *42*, 70–74.
26. Li, D.; Lu, X.; Zhao, X. Experimental Study on Low Pressure Jet Characteristic of the Non-circle Jet Nozzle. *Light Ind. Mach.* **2006**, *24*, 18–20.
27. Zhou, X.; Li, H.; Jiang, Y. Study on water distribution uniformity of non-circular nozzles at low pressure. *J. Drain. Irrig. Mach. Eng.* **2017**, *35*, 448–453.
28. Jiang, Y.; Li, H.; Hua, L.; Zhang, D.; Issaka, Z. Experimental Study on Jet Breakup Morphologies and Jet Characteristic Parameters of Non-Circular Nozzles under Low-Intermediate Pressures. *Appl. Eng. Agric.* **2019**, *35*, 617–632. [[CrossRef](#)]
29. Liu, X. Droplets Distribution Characteristic Study on Complete Fluidic Sprinkler. Master's Thesis, Jiangsu University, Zhenjiang, China, 2016.
30. Zhu, X.; Shi, Y.; Hu, G.; Liu, J. Dynamic Simulation and Test of Water Distribution of Fluidic Sprinkler. *J. Irrig. Drain.* **2020**, *39*, 74–83. [[CrossRef](#)]
31. Zhu, X.; Liu, G.; Liu, J.; Jiang, J.; Tian, K. Droplets distribution research of impact sprinkler based on Laser Precipitation Monitor. *J. Drain. Irrig. Mach. Eng.* **2015**, *33*, 908–914.
32. Liu, J.; Yuan, S.; Li, H.; Zhu, X. Analysis and Experiment on Influencing Factors of Range and Spraying Uniformity for Complete Fluidic Sprinkler. *Trans. Chin. Soc. Agric. Mach.* **2008**, *39*, 51–54.